

Performing Quantitative Nanomechanical AFM Measurements on Live Cells

Bede Pittenger* and Andrea Slade

Bruker Nano Surfaces, 112 Robin Hill Road, Santa Barbara, CA 93117

*bede.pittenger@bruker-nano.com

Introduction

Atomic force microscopy (AFM) has been recognized since the mid-eighties [1] as an excellent technique to image a wide range of samples in their near-natural environment. Although the primary function of AFM is to generate three-dimensional (3D) profiles of the scanned surface, much more information can be delivered via this technique. In 1993, TappingMode was developed [2], which prevents tip and sample damage due to friction and shear forces and allows qualitative mechanical property mapping through phase imaging [3, 4]. About the same time, force spectroscopy [5] and force volume (FV) [6] were developed to study tip-sample forces at a point or over an area, respectively. To date, force spectroscopy and FV are the most commonly used AFM modes for measuring nanometer-scale mechanical forces in a quantitative manner. Unfortunately, force spectroscopy and FV suffer from slow acquisition speed and a lack of automated tools; these operating characteristics limit their use because of the hundreds or thousands of curves that are required for good statistics.

In 2010, the PeakForce QNM mode was developed [7], based on Bruker's PeakForce Tapping technology. In this technique, the probe is oscillated around 1 kHz and the peak force (maximum nominal force applied to the sample) is used for feedback control. Each time the tip interacts with the sample, a force curve is collected and analyzed by PeakForce QNM. The resulting signals are extracted and quantitatively displayed as a false-colored, real-time image. Currently available data types include the peak force, the adhesion, the Young's modulus, the deformation, and the dissipation. This mode has been successfully tested on a wide range of samples [8], including bio-polymers [9, 10] and live eukaryotic cells [11], as well as human models [12]. This article describes the application of this method to measurements on live cells.

Comparing FV and PeakForce QNM

Because measuring and mapping mechanical properties of live samples are of high importance in biology, the capabilities of force spectroscopy, FV, and PeakForce QNM AFM are all useful for studying cell mechanics. Table 1 summarizes the characteristics of each technique and compares their principal benefits and drawbacks. PeakForce QNM is best for high-resolution imaging or relatively high-speed imaging where material properties are of interest. FV is useful as a comparison to PeakForce QNM and for cases where the loading rate dependence of the measurement is important, such as studies of viscoelastic behavior and kinetic binding or unfolding measurements. Single-point force spectra are best for situations where mapping is not as important, where there are only a few points of interest in a sample, or where force measurements need to be separated by some distance to avoid the interaction

of one measurement with the next. The key differences between PeakForce QNM and the more traditionally used FV (and force spectroscopy) are:

1. PeakForce QNM uses a sinusoidal modulation of the base of the cantilever relative to the sample surface, whereas FV uses linear ramping. This allows PeakForce QNM to acquire thousands of ramps per second, whereas FV ramping is usually limited to a maximum of around ten ramps per second. The higher ramp rate of PeakForce QNM permits the acquisition of more detailed material property maps in much less time than FV.
2. PeakForce QNM controls the normal force of the tip-sample interaction by detecting the peak force of each tap and feeding the information into a feedback loop that is running continuously. This force control benefits from the results of previous taps and from the fact that the sinusoidal waveform causes the tip velocity to approach zero as the tip approaches the peak, allowing for an ultra-low interaction force (the peak force can be as low as ten pN). This is in contrast to FV where each tap is treated separately and the tip approaches the surface at full speed. Once the trigger force is detected, the system attempts to retract instantaneously, leading to overshoot and larger forces, especially at higher ramp rates.
3. PeakForce QNM is usually more stable than FV because there is less time for the system to drift within an image, and because the superior force control inhibits tip wear and contamination.

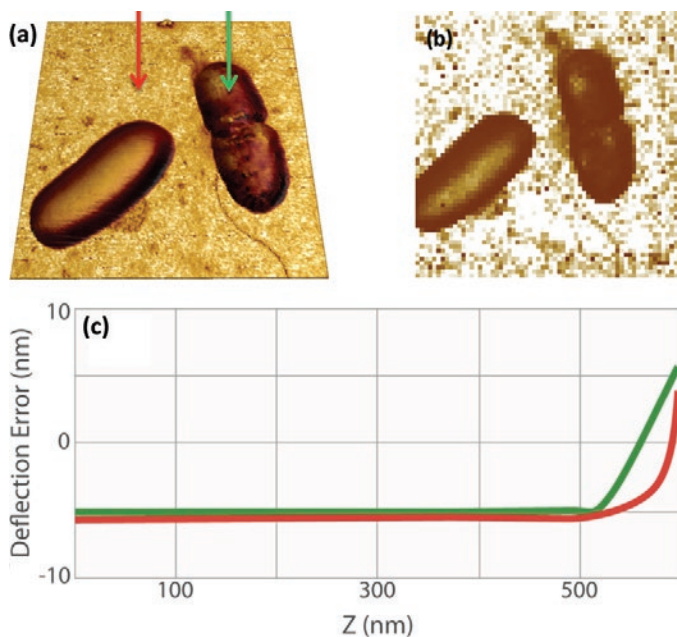
These properties make PeakForce QNM significantly better for material property mapping than FV in most cases. On the other hand, FV and force spectroscopy allow more control of the details of the ramp, such as independent control of approach and retract tip velocities and surface hold. Also, FV and force spectroscopy taps can be separated by some distance because the triggering is treated independently, whereas PeakForce QNM taps must be close together in order to achieve the best feedback performance.

Results

Preliminary testing on bacteria. Figure 1a shows a pair of *E. coli* bacteria rendered in 3D, based on the topography of the sample, with the brightness of the image based on the value of Young's modulus. This image was collected using PeakForce QNM in about 10 minutes. This is in contrast to the FV image in Figure 1b, which took about 35 minutes to collect. The improvement in speed is convenient and allows more and higher-resolution images (in this case, 256×256 versus 64×64) to be collected during the life of a cell. The bacteria are

Table 1: The advantages and disadvantages of FV, PeakForce QNM, and single-force measurements. A description of each technique and its ideal use case is also given.

	PeakForce QNM	Quantitative Force Volume	Single-Force Curves
Measurement	Sinusoidal force curves are measured during scanning. Continuous feedback loop controls tip-sample force. Property maps are generated in real-time.	Single-force curves are measured at points on 2D grid. Tip-sample force is controlled by triggering at each point. Property maps are generated in real-time.	Single-force curves are measured at discrete points. Tip-sample force is controlled by triggering at each point. Spatially targeted using AFM or optical images
Benefits	Fastest high-resolution property mapping Feedback-controlled sinusoidal drive Direct and precise force control Force curves are available for offline analysis.	Highly accurate force measurements Widely accepted technique	Highly accurate force measurements Spatially targeted using AFM or optical images
Disadvantages	To look at a sample with lower resolution, some data points must be removed.	Typically lower-resolution mapping with slower acquisition rates Increased ramp rates results in overshooting force trigger.	No real-time property mapping
Ideal Case Use	High-speed, high-resolution property mapping High-frequency response for viscoelastic studies	Low-frequency response for viscoelastic studies Loading rate dependence (e.g., unbinding/unfolding kinetics)	Discretely targeted force measurements Low-frequency response for viscoelastic studies Loading rate dependence (e.g., unbinding/unfolding kinetics)

**Figure 1:** (a) PeakForce QNM (250 Hz) Sneddon modulus data painted on 3D topography of *E. coli* bacteria. Brighter areas are stiffer, with the brightest areas in the substrate about 50 MPa. (b) FV Sneddon modulus image of the same bacteria collected at a ramp rate of 2 Hz. (c) Two force curves from the Peak Force Capture file showing the difference between substrate and cell. (Standard DNP-A probe in water with 300 nm modulation amplitude, scan size = 5 μm .)

still alive during imaging (in liquid at room temperature), and the one on the right appears to be in the process of dividing. Note that the dividing cell on the right is significantly softer (darker) than the cell on the left (~2 MPa versus ~15 MPa). Note the presence of some softer components on the substrate, including the bacterial flagella in the lower-right corner. For these images, the modulus was calculated using the Sneddon (conical) model [3], assuming a tip with an 18-degree half-angle (typical for the DNP-A type probe used).

It is useful to examine individual force curves from interesting parts of the image. PeakForce Capture allows the simultaneous capture of the force curves that were used to create the property maps in PeakForce QNM. As before, QNM images are still acquired normally, but a force curve for each pixel in the property map is saved separately in a Quantitative Force-Volume file format. These files can be opened in NanoScope analysis for additional exploration with the full Quantitative Force-Volume analysis tools. Additionally, calibration parameters can be adjusted and different property models can be compared (for example, Sneddon [13] versus the Derjaguin-Muller-Toporov (DMT) [14]). Because the same tools are used to analyze both FV and PeakForce Capture files, it is simple to compare results collected at ramp rates from 0.1–10 Hz (FV) to those at ramp rates from 250 Hz and higher (PeakForce Capture). This allows investigation of the time dependence of the tip-sample interaction.

Figure 1c shows a pair of force curves (approach only) from PeakForce Capture. One was collected on top of the cell, whereas the other was collected on the sample substrate as indicated in Figure 1a. The slope of the curve from the substrate (red) is initially smaller than that of the bacteria, but it increases rapidly, becoming nearly vertical at the most extended point. This occurs because there is a soft, thin gelatin coating on the substrate that is intended to aid immobilization [15] of the bacteria cells. When the tip penetrates deeper into the gelatin, it begins to feel the underlying glass substrate, which is much stiffer than the cells. The curve collected on the cell (green) is more uniform in slope, indicating that the substrate is not influencing the measurement significantly.

Probing agarose gels at various ramp rates. Agarose is a polysaccharide derived from agar. It is most widely used as a medium for gel electrophoresis measurements, but it is appearing in recent applications as a tissue mimicking material (for example, tissue phantoms) [16–19]. The mechanical properties of agarose gels are concentration-dependent, with higher agarose concentrations resulting in “stiffer” gels. This allows preparation of agarose gels having different elastic modulus values in the biologically relevant range of tens to thousands of kilopascal (kPa). To demonstrate the ability of FV and PeakForce QNM to measure these very soft samples, gels containing 1%–5% by wt. of agarose were prepared and imaged in phosphate buffered saline (PBS) buffer. Figure 2a shows typical approach curves collected on the 3% agarose sample with ramp rates from 1 Hz (FV) to 250 Hz (PeakForce QNM) are overlaid on the same plot to demonstrate the similarity of results from the two techniques even over several orders of magnitude of ramp rate. If Sneddon modulus is calculated for each of these curves, the results were 353 kPa at 1 Hz, 340 kPa at 5 Hz, 357 kPa at 10 Hz, and 351 kPa at 250 Hz. These results are essentially identical within the uncertainty of the measurement.

Figures 2b, 2c, and 2d show the same type of experiment in a more statistically relevant way. The FV results (1 Hz) are shown in green with the PeakForce QNM results at 250 Hz in red. The PeakForce QNM histogram provides much better statistics because it is based on 16,384 (128×128) measurements compared to 256 (16×16) measurements for FV. Despite the large difference in the number of samples for each measurement, the acquisition times are similar: ~11 minutes for PeakForce QNM versus 4 minutes for FV. Thus, PeakForce QNM provides significantly better statistics than FV at minimal cost. The Young's modulus can be calculated by directly analyzing the color contrast of the captured images (bearing analysis) or by exporting and processing the selected force curves. When thousands of curves are involved, automated analysis becomes critical.

If the sample has a significant time-dependent deformation mechanism such as viscoelasticity, the results of FV and PeakForce QNM may be different, because the time dependence allows different amounts of deformation within the time scale of the ramp. Figures 2b, 2c, and 2d show that there is very little difference between measurements at 250 Hz (PeakForce QNM) and 1 Hz (FV) for the 1% and 3% gels, but the 5% gel has some increase in modulus at higher frequencies. Note that the Sneddon and DMT models only include elastic

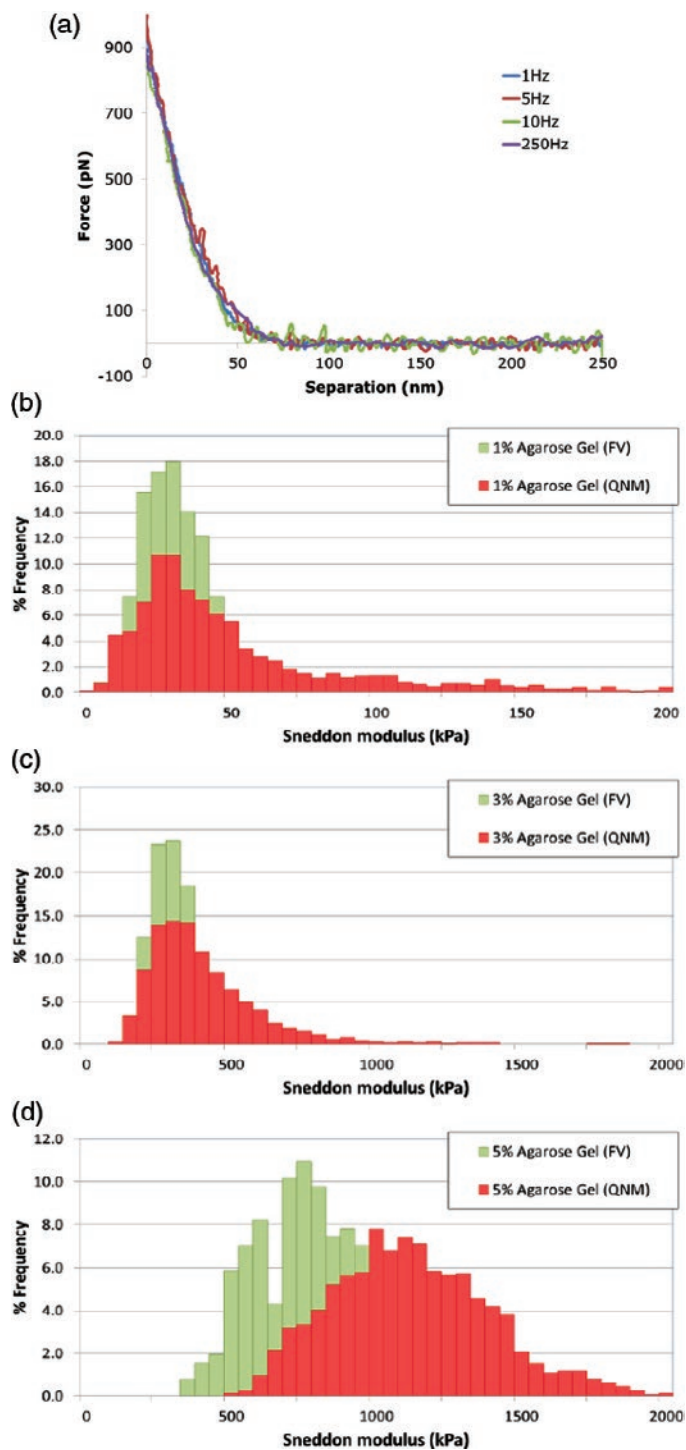


Figure 2: Agarose gels at different ramp rates: (a) Individual curves collected on 3% agarose gel at different ramp rates between 1 Hz and 250 Hz. (b, c, d) Histograms of Sneddon modulus results on 1%, 3%, and 5% agarose gel, respectively, comparing ramp rates of 1 Hz with FV (green) and 250 Hz with PF-QNM (red). MLCT-D probe, $k = 0.047$ N/m, 1 nN trigger, ramp size: 300 nm.

deformation mechanisms (without time dependence). To quantify this time-dependent behavior, new analysis techniques are needed.

FV versus PeakForce QNM on live cells. Many phenomena relating to the lifecycle and behavior of cells (for example, cancer cells) are related to cell mechanics or

the mechanics of the constituent parts of the cell. The faster, higher-resolution mapping made possible with PeakForce QNM allows more detailed mapping of these processes as they occur. The limited duration of these processes and cell lifetimes make speed of acquisition a critical aspect of many experiments. Figure 3 demonstrates the resolution possible on the lamellipodium of a mouse B16 cell imaged in HEPES buffer. This image was collected in 8.5 minutes; a similar FV map collected at a ramp rate of 2 Hz with the same resolution would take about 9 hours.

Figure 3a shows a 3D topographic rendering of the lamellipodium showing some actin fibrils. Figures 3b and 3c compare modulus maps calculated from the DMT (sphere) model using the retract curves and the Sneddon (cone) model using the approach curves. The substrate image (upper right) is saturated to white because the cantilever spring constant for the probe used is too small to provide a quantitative modulus measurement on the much stiffer surface of the glass bottom Petri dish. The DMT modulus map is brighter than in the Sneddon map, which we expect to be more accurate because the deformation depth on the cell was between 100 and 200 nm. Because the tip radius is ~ 30 nm, the tip shape can be approximated by that of a cone. To demonstrate the difference, a single curve was extracted from the PFC data and analyzed with both the DMT model (b) and the Sneddon model (c). Comparing the green fit curve to that of the data, it is easy to see that the Sneddon model fits the data much better than the DMT model.

During image acquisition, force curves (similar to those in Figures 3b and 3c) were collected and analyzed along with the topography, providing the simultaneous maps of DMT modulus, Sneddon modulus, peak force error, deformation, dissipation, and adhesion. Figure 4 shows six examples of these

maps. Details such as the actin fibrils in the cell cytoskeleton are visible in many of the channels, but there are differences. For example, the Peak Force Error channel and Deformation channel show many small fibrils, whereas fewer fibrils are visible in the modulus channels and none are visible in the adhesion map.

Although PeakForce QNM can correct for some background deflection not related to the short-range tip-sample interaction, it is not always possible to correct all of the background in fluid due to variation of apparent liquid viscosity near the sample surface. For highest measurement accuracy, it is best to minimize this viscous background by using the smallest modulation amplitude possible and <1 kHz modulation frequency. These images were collected with modulation amplitude of 200 nm at 250 kHz. The probe was also selected with the viscous background in mind.

FV is well accepted as a tool for studying the mechanical properties of cells at ramp rates of less than 10–20 Hz. Figure 5 compares the Sneddon modulus maps from Figure 3 with those from FV at 1 Hz and 5 Hz and with PeakForce Capture at 250 Hz. All of the maps show that the cell's lamellipodium has about the same modulus (compare the color of the lower-left part of each image in Figures 5a and 5b) independent of ramp rate and technique. Figure 6 shows a histogram of all of the images, showing that all of the peaks are around 20 kPa (0.02 MPa). The lack of variation indicates that there is little viscoelasticity or any other time-dependent deformation mechanism active in the range of frequencies between 1 Hz and 250 Hz for the lamellipodium of this cell. The FV images were collected at low resolution (16×16 pixels) to save time, but the resulting modulus maps do not have enough resolution to clearly identify the actin fibrils in the cytoskeleton that are visible in the PFC and PF-QNM images.

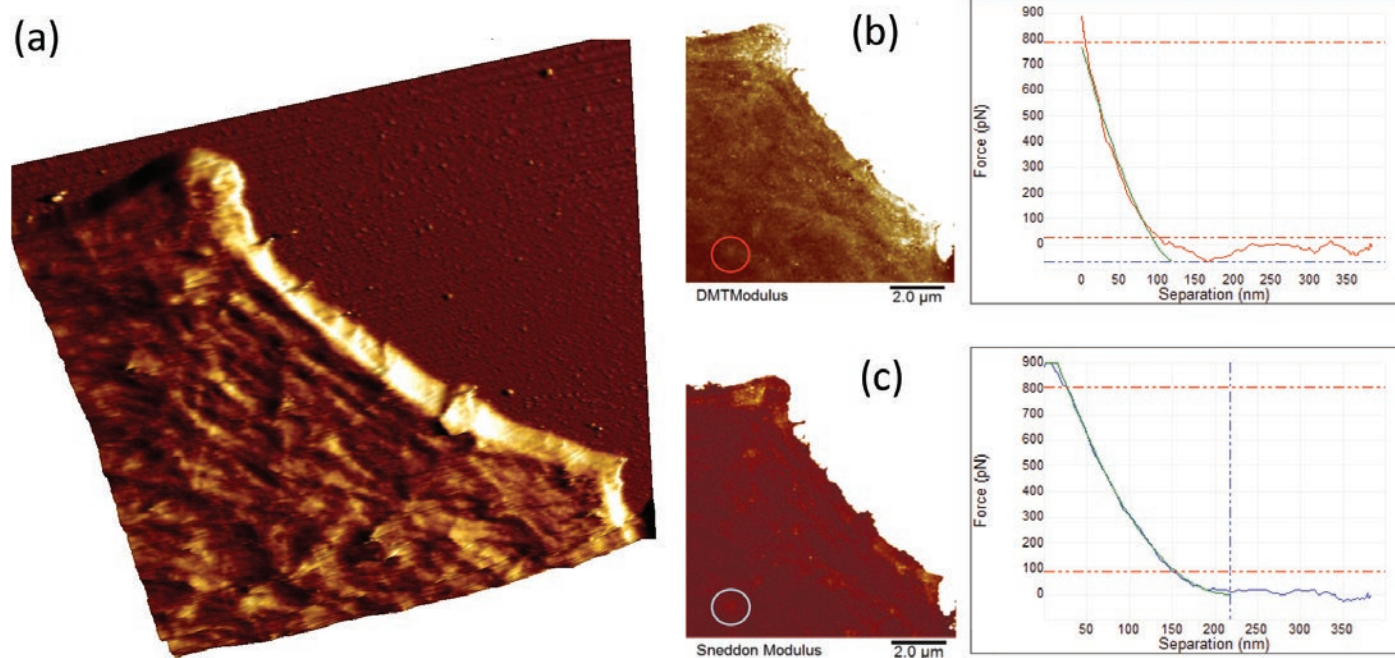


Figure 3: Lamellipodium of a mouse B16 cell imaged in HEPES buffer: (a) 3D rendering of the lamellipodium topography showing actin fibrils. (b–c) Comparison between maps of DMT modulus and Sneddon modulus, along with individual curves and fits (DMT model fit results in a modulus of 50 kPa, Sneddon model fit results in 37 kPa) from the same point in the image. (Classic MLCT-D $k = 0.048$ N/m, tip with 35-degree half-angle, $R \sim 50$ nm end radius, modulation amplitude of 200 nm at 250 kHz to minimize viscous background, setpoint 1 nN.)

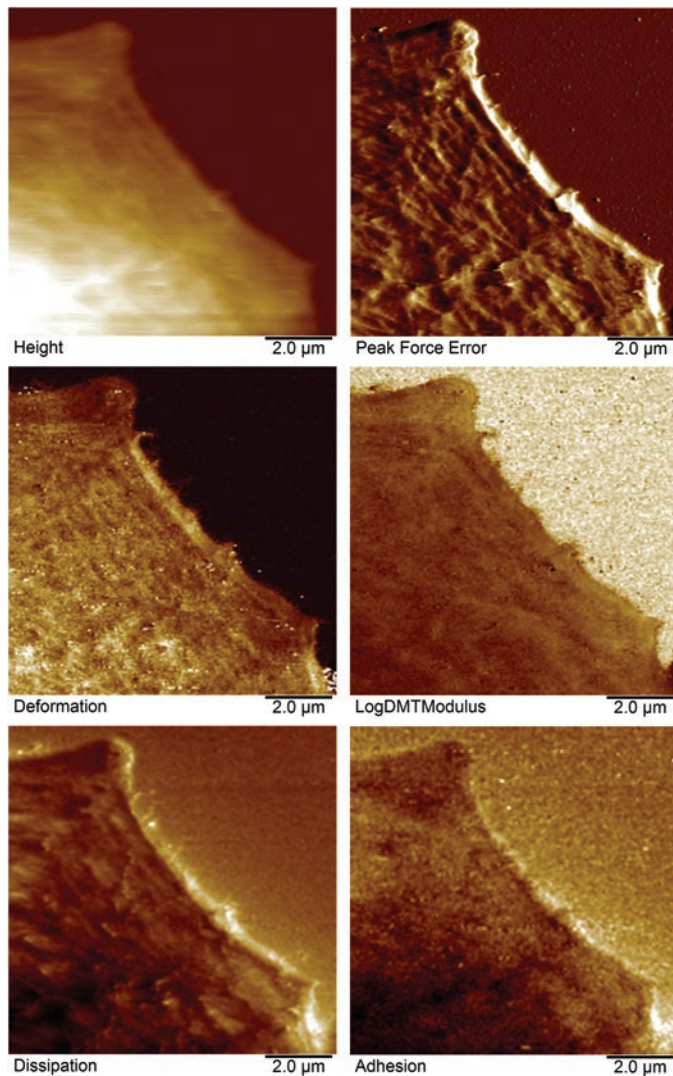


Figure 4: Six data channels, collected simultaneously with Figure 3, mapping the properties of the cell, such as height, peak force error, deformation, log DMT modulus, dissipation, and adhesion.

Conclusion

The mechanical properties of biological samples often affect their structure and functional activity and are hence important to biologists. FV has been accepted since the mid 1990s and is still a powerful tool for measuring and mapping the mechanical properties of biological samples. FV is optimized for mapping with low ramp rates (~0.5–10 Hz) and relatively low resolution. PeakForce QNM improves upon FV in terms of resolution and speed (with ramp rates ~250 Hz–2 kHz), making it more practical to collect and analyze significantly more data for better detail and statistics. Together, FV and PeakForce QNM provide opportunities for comparisons of material response over about four orders of magnitude of ramp rate in air or in a liquid environment.

Special thanks to Manfred Radmacher (University of Bremen, Germany) for assistance with the mouse cell measurements.

References

- [1] G Binnig, CF Quate, and C Gerber, *Phys Rev Lett* 56 (1986) 930–33.

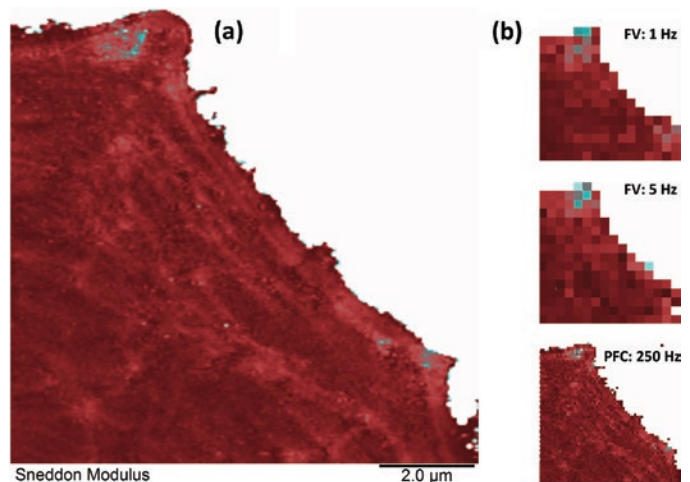


Figure 5: Comparison of Sneddon modulus values obtained with PF-QNM and FV at two different ramp rates: (a) 256×256 pixel map of Sneddon modulus calculated simultaneously with topographic imaging. Note that actin fibrils are visible in the cytoskeleton. (b) FV images at 1 Hz (top), 5 Hz (middle), and PFC image at 250 Hz (bottom). All images are plotted with the same data scale and color bar with a range of -50 to +300 kPa for all.

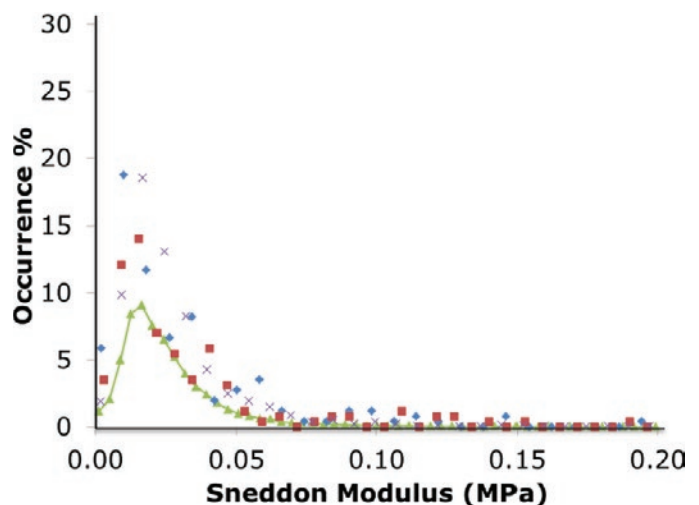


Figure 6: Histogram of modulus on the lamellipodium at different ramp rates. Green line is from 250 Hz PeakForce QNM image, blue diamonds are FV at 5 Hz, red squares are FV at 1 Hz, Xs are from 250 Hz PeakForce Control data calculated offline.

- [2] Q Zhong, D Innis, K Kjoller, and VB Elings, *Surf Sci* 290 (1993) 688–92.
- [3] DA Chernoff, “High Resolution Chemical Mapping Using Tapping Mode AFM with Phase Contrast,” in *Proceedings Microscopy and Microanalysis*, ed. GW Bailey, Jones & Begell Publishing, Redding, CT, 1995, 888–89.
- [4] J Tamayo and R García, *Langmuir* 12 (1996) 4430–35.
- [5] GU Lee, DA Kidwell, and RJ Colton, *Langmuir* 10 (1994) 354–57.
- [6] M Radmacher, JP Cleveland, M Fritz, HG Hansma, and PK Hansma, *Biophys J* 66 (1994) 2159–65.
- [7] B Pittenger, N Erina, and C Su, “Quantitative Mechanical Properties Mapping at the Nanoscale with PeakForce QNM,” *Bruker Application Note* #128 (2011).

- [8] A Berquand, "Quantitative Imaging of Living Biological Samples by PeakForce QNM," *Bruker Application Note* #135 (2012).
- [9] J Adamcik, A Berquand, and R Mezzenga, *Appl Phys Lett* 98 (2011) 193701-03.
- [10] TJ Young, MA Monclus, TL Burnett, WR Broughton, SL Ogin, and PA Smith, *Meas Sci Technol* 22 (2011) 125703.
- [11] G Pletikapic, A Berquand, T Mistic, and V Svetlicic, *J Physcol* 48 (2012) 174-85.
- [12] C Heu, A Berquand, C Caille-Elie, and L Nicold, *J Struct Biol* 178 (2012) 1-7.
- [13] IN Sneddon, *Int J Eng Sci* 3 (1965) 47-57.
- [14] B Derjaguin, V Muller, and Y Toporov, *J Colloid Interf Sci* 53 (1975) 314-26.
- [15] MJ Doktycz et al., *Ultramicroscopy* 97 (2003) 209-16.
- [16] B Luo, R Yang, P Ying, M Awad, M Choti, and R Taylor, in *Proceedings of IEEE 32nd Annual Northeast Bioengineering Conference*, IEEE, Piscataway, NJ, 2006, 81-82.
- [17] D Lobsien, AY Dreyer, A Stroh, J Boltze, and K-T Hoffmann, *PLoS One* 8 (2013) e62644.
- [18] R Deepthi, R Bhargavi, K Jagadeesh, and MS Vijaya, *SASTECH* 9 (2010) 27-30.
- [19] S Pichardo, J Kivinen, D Melodelima, and L Curiel, *Phys Med Biol* 58 (2013) 2163-83.

MT

PELCO® Silicon Nitride & Silicon Dioxide Membranes

Next Generation SiN TEM Support Films

- Robust and clean 8, 15, 50 and 200nm SiN substrates
- ø3.0mm frame
- EasyGrip™ edges
- Free from debris
- Super flat 8, 15, and 40nm silicon dioxide substrates




Holey SiN Substrates

Silicon Dioxide Substrates



TED PELLA, INC.
Microscopy Products for Science and Industry

www.tedpella.com sales@tedpella.com 800.237.3526

BREAKTHROUGH TO BEST IN CLASS SPUTTERING ON YOUR DESKTOP



The Desktop Pro, a compact, high vacuum sputtering system for research, production support and sample preparation.

DENTON VACUUM
BARRIERS BECOME BREAKTHROUGHS

Visit our new website

www.dentonvacuum.com/mt